Proposed Thermodynamic Pressure Scale for an Absolute HighPressure Calibration

D. L. Decker and J. D. Barnett

Articles you may be interested in

Calibration of Sm:YAG as an alternate highpressure scale
J. Appl. Phys. **68**, 5357 (1990); 10.1063/1.347031

Highpressure calibration with a new absolutepressure gauge
Appl. Phys. Lett. **22**, 310 (1973); 10.1063/1.1654650

HighPressure Calibration: A Critical Review
J. Phys. Chem. Ref. Data **1**, 773 (1972); 10.1063/1.3253105

Calibration of High-Pressure Ionization Gauge
J. Vac. Sci. Technol. **5**, 152 (1968); 10.1116/1.1492603

Sonar Transducer Calibration in a HighPressure Tube
J. Acoust. Soc. Am. **39**, 48 (1966); 10.1121/1.1909873

TABLE I. Comparison of analog computer solutions with the results of Chen[2]; first-order thermoluminescence glow curves with constant s.

E (eV)	s (sec^{-1})	T_m (°K) This work	T_m (°K) Ref. 2	T_m (°K) % diff.	Full width (°K) This work	Full width (°K) Ref. 2	Full width (°K) % diff.
0.1	10^{13}	37.0	37.6	1.6	2.8	2.8	0.0
0.2	10^{13}	73.5	73.7	0.3	5.6	5.5	0.2
0.4	10^{13}	145.2	144.5	0.5	10.2	10.6	4
0.8	10^{13}	295.8	283.2	4.4	21.6	20.3	6
0.1	10^{11}	42.9	43.8	2.1	3.75	3.9	5
0.2	10^{11}	85.6	85.4	0.2	7.5	7.3	3
0.4	10^{11}	166.8	166.9	0.1	14.0	14.0	0.0
0.8	10^{11}	340.0	326.2	4.2	28.5	26.7	7
0.1	10^{9}	52.5	52.1	0.8	5.3	5.4	2
0.2	10^{9}	101.4	101.3	0.1	10.8	10.3	5
0.4	10^{9}	200.4	197.2	1.6	19.8	19.9	0.5
0.8	10^{9}	403.0	383.9	5.0	34.5	36.8	6
0.1	10^{7}	64.5	64.2	0.5	8.35	8.2	2
0.2	10^{7}	124.4	124.1	0.2	16.2	15.2	6
0.4	10^{7}	250.0	240.1	4.1	30.8	28.5	8

scaled with the computer variable proportional to n and machine time proportional to temperature. The patching of (3) on an EAI TR-20 analog computer was conventional and required 4 integrators, 3 "quarter square" multipliers or dividers, 17 operational amplifiers, and 6 potentiometers. A typical solution for $E=0.4$ eV and $s=10^9$ sec^{-1} as drawn directly by a Moseley Type 2S X-Y plotter is shown in Fig. 1. The results obtained for the peak temperature T_m and the full width at one half peak intensity are compared with the results of Chen[1] in Table I for 0.1 eV$\lesssim E \lesssim 0.8$ eV and 10^7 sec$^{-1}\lesssim s \lesssim 10^{13}$ sec^{-1}. The maximum discrepancy in E is 5% and somewhat higher for the width parameter. The larger differences probably result from termination errors in the asymptotic expansion used by Chen[1] plus systematic errors in the analog computer integrations. The overall good agreement shows that analog computer calculation of TL glow curves directly from the differential equation is a feasible procedure, and the method can be extended readily to more complicated kinetics models.

The quantity n_0 which occurs as a scaling factor in (2) is closely related to the "light sum" L by

$$L = \int_0^\infty I\,dt = Cn_0. \tag{4}$$

In comparing solutions for the same value of n_0 and β it was noted that the peak intensity I_m is related to T_m in a systematic way, as shown in Fig. 2. The parallel lines for each trap depth indicate an accurate $T_m^{-2.03}$ dependence independent of s, while the vertical displacement of each line is directly proportional to E. Since the peak TL intensity is not usually considered as a parameter in glow curve analysis, it is interesting to explore the origin of this correlation. The asymptotic expansion used in the analysis of Grossweiner[3] leads to:

$$\int_0^{T_m} \exp\left(\frac{-E}{kT}\right) dT = T_m \exp\left(\frac{-E}{kT_m}\right) + \frac{E}{k} Ei \frac{-E}{kT_m}$$

$$\simeq \frac{kT_m^2}{E} \exp\left(\frac{-E}{kT_m}\right), \tag{5}$$

where

$$Ei(-x) = \int_x^\infty \frac{e^{-u}}{u} du.$$

The substitution of (5) in (2) for $T = T_m$ and the elimination of (s/β) by setting the derivative of (1) equal to zero leads to

$$I_m = C(dn/dt)_m = C(n_0 E\beta/ekT_m^2), \tag{6}$$

where e is the base of natural logarithms. Thus, the correlation in Fig. 2 follows directly from (6) except for the small difference in the T_m exponent, which probably results from the termination error in (5). A possible application would be in the determination of E from the light sum L and T_m, where Cn_0 can be eliminated with (4), although this procedure is probably less convenient than the Grossweiner[3] method which requires only T_m and the low-temperature-side halfwidth. However, (6) may be useful in planning of TL experiments where the required detection sensitivity can be related to the trapping parameters.

[1] J. J. Randall and M. H. F. Wilkins, Proc. Roy. Soc. (London) A184, 366, 390 (1945).
[2] R. Chen, J. Appl. Phys. 40, 570 (1969).
[3] L. I. Grossweiner, J. Appl. Phys. 24, 1306 (1953).

Proposed Thermodynamic Pressure Scale for an Absolute High-Pressure Calibration

D. L. DECKER AND J. D. BARNETT
Department of Physics and Astronomy, Brigham Young University, Provo, Utah 84601

The field of high pressure has developed rapidly over the past few years to a point where relatively sophisticated experiments are being attempted. In many experiments it is no longer sufficient to qualitatively estimate the pressure or to base conclusions on experimental results tied to an empirical pressure parameter. One desires to accurately know the pressure dependence of physical quantities related to a true thermodynamic scale. A fundamental pressure measurement must be directly or indirectly tied to a measurement of f/α, where f is the force exerted on an area α, or to a measurement of $-(\partial F/\partial V)_T$ where F is the

TABLE I. Possible accuracy of pressure measurements at selected values of pressure using NaCl.

Pressure	8 kbar	25 kbar	55 kbar	77 kbar
(σ_p/P)	1.4×10^{-2}	5.8×10^{-3}	4.1×10^{-3}	3.7×10^{-3}
δ	0.11 kbar	0.14 kbar	0.22 kbar	0.29 kbar
Present accuracy[a]	0.002 kbar	0.06 kbar	1 kbar	2 kbar

[a] These values were determined at the Symposium on the Characterization of the High Pressure Environment, National Bureau of Standards, Oct. 1968.

Helmholtz free energy at volume V and temperature T. In practice, accurate high-pressure measurements based on

$$P = f/\alpha, \qquad (1)$$

and using the piston–cylinder technique, are hampered by internal friction in the pressure-transmitting medium surrounding the sample, friction between the piston and cylinder, and distortion of the piston under stress, whose area must be determined. These corrections, which must be applied to the measurement, are usually difficult to determine accurately and cannot, in general, be unambiguously determined experimentally, but normally involve theoretical approximations. The other approach,

$$P = -(\partial F/\partial V)_T, \qquad (2)$$

is also difficult experimentally because one does not usually known how to measure the free energy. Theoretical attempts to evaluate F for particular materials have proven useful to obtain a practical pressure scale.[1,2]

We propose to obtain a thermodynamic pressure scale following a well-known technique often applied in the case of the thermodynamic temperature scale.[3] If a set of physical quantities, which are related by a thermodynamic relationship involving the thermodynamic pressure, can all be separately measured as functions of an empirical pressure parameter, then the thermodynamic relation can be used to express the thermodynamic pressure as a function of this same empirical pressure parameter. By empirical pressure parameter we mean any physical measurable quantity which is reproducible and varies monotonically with pressure. (For our purposes we also desire this parameter to have the value zero at $P=0$.) An example of such a parameter is the change in the electrical resistance of a properly prepared manganin wire in a hydrostatic pressure medium.

Consider the thermodynamic relations[4]

$$B_T = -V(\partial P/\partial V)_T = B_s + \alpha^2 V^2 B_s T(\partial P/\partial V)_T/C_p, \qquad (3)$$

where B_T and B_s are the isothermal and abiabatic bulk moduli, respectively, $\alpha = 1/V(\partial V/\partial T)_p$ is the volume thermal expansion coefficient, and C_p is the specific heat at constant pressure. These equations can be solved for $(\partial P/\partial V)_T$ yielding

$$(\partial P/\partial V)_T = -B_T/V = -B_s/[V(1+\alpha^2 V B_s T/C_p)]. \qquad (4)$$

Let Π represent the value of some empirical pressure parameter and suppose that B_T and V or B_s, V, α, and C_p can be measured as functions of Π. We then integrate Eqs. (4) along an isotherm to get

$$P(\Pi) = -\int_0^\Pi \frac{B_T}{V}\left(\frac{\partial V}{\partial \Pi}\right)_T d\Pi = -\int_0^\Pi \frac{B_s(\partial V/\partial \Pi)_T d\Pi}{V(1+\alpha^2 V B_s T/C_p)}. \qquad (5)$$

These are expressions for the thermodynamic pressure P as a function of Π, and once the terms in the integrand have been measured over a range of the parameter Π then $P(\Pi)$ is experimentally known and the empirical pressure parameter has been calibrated in terms of the true thermodynamic pressure.

Before Eq. (5) can be proposed as a usable pressure calibration technique, we must consider the accuracy attainable by this method of measuring $P(\Pi)$. B_s can be measured using ultrasonic techniques to an absolute accuracy of 2 parts in 10^3 or even better with some materials. Volume measurements are presently accurate to 1 part in 10^3 and could likely be improved by an order-of-magnitude in a hydrostatic medium (which is now possible to 60 kbar).[5] Measurements of α are only accurate to a few percent and an accurate measurement of C_p at high pressure would be rather difficult. Fortunately, $\alpha^2 V B_s T/C_p = \alpha\gamma T \ll 1$, and is 0.05 for NaCl, for example, near room temperature. (γ is the Gruneisen parameter.) The quantity $\alpha\gamma T$ can be measured at atmospheric pressure with an accuracy approaching 3% and it decreases slowly with pressure such that one can estimate the value of $1+\alpha\gamma T$ at elevated pressures with nearly the same accuracy as at atmospheric pressure. Thus we can use the first integral in Eq. (5) determining $B_T = B_s/(1+\alpha\gamma T)$ with an absolute accuracy of about 3 parts in 10^3 and a statistical scatter possibly as small as 5 parts in 10^5.

In order to estimate the accuracy in the measurement of $P(\Pi)$ by this method we replace the integral in Eq. (5) by a sum.

$$P = -\sum_{k=1}^{n} B_k\left(1 - \frac{V_{k-1}}{V_k}\right), \qquad (6)$$

where B_k and V_k specify the n individual measurements of B_T and V at various values of Π. Now

$$(\delta P)^2 = \sum_{k=1}^{n} \frac{B_k^2(V_k - V_{k-1})^2}{V_k^2}\left(\frac{\delta B_k}{B_k}\right)^2 + \left(\frac{B_1 V_0}{V_1}\right)^2\left(\frac{\delta V_0}{V_0}\right)^2$$
$$+ \left(\frac{B_n V_{n-1}}{V_n}\right)^2\left(\frac{\delta V_n}{V_n}\right)^2 + \sum_{k=1}^{n-1}\left(\frac{B_{k+1}V_k}{V_{k+1}} - \frac{B_k V_{k-1}}{V_k}\right)^2\left(\frac{\delta V_k}{V_k}\right)^2, \qquad (7)$$

where we have assumed all B_k and V_k are statistically independent, which would not include any systematic errors in their measurement. In order to simplify Eq. (7), we assume $\delta B_k/B_k = \sigma_B/B$ and $\delta V_k/V_k = \sigma_v/V$ for all k, B_k increases nearly linearly with pressure, and that the measurements are sufficiently closely spaced so that $V_{k-1}/V_k = 1$. Then

$$\frac{\sigma_p}{P} \cong \left[\left(\frac{s_B}{B}\right)^2 + \frac{1}{n}\left(\frac{\sigma_B}{B}\right)^2 + \frac{B_n^2 + B_0^2}{P^2}\left(\frac{\sigma_v}{V}\right)^2\right]^{1/2}, \qquad (8)$$

where we have introduced s_B/B to account for systematic errors in the measurement of B_T. We note that any systematic errors in the measurement of V will cancel.

Let $s_B/B = 3\times10^{-3}$, $\sigma_B/B = 5\times10^{-5}$, and $\sigma_v/V = 3\times10^{-4}$, and assume that measurements of B_T and V are made at intervals of 1 kbar using a sample of NaCl. The uncertainty in the measured pressure is then given in Table I at selected pressures. These pressures were chosen in that they correspond to the equilibrium value of the transitions in Hg, Bi, and Ba which are commonly used as high pressure calibration points. The final row of the table gives the accuracy of the best measurement of these points to date. The data in the table demonstrate that the proposed technique does not compete with the free piston gauge below 10 kbar but is comparable near 25 kbar. Above 25 kbar this technique is considerably more accurate than the piston–cylinder apparatus, providing a hydrostatic environment is available and

ultrasonic measurements can be extended into this range. It is interesting that the % error using this technique decreases as we get to higher pressures approaching a limiting value which is set by the absolute accuracy of the determination of the isothermal bulk modulus.

[1] D. L. Decker, J. Appl. Phys. **36**, 157 (1965); R. N. Jeffery, J. D. Barnett, H. B. Vanfleet, and H. T. Hall, J. Appl. Phys. **37**, 3172 (1966).

[2] D. J. Pastine, Phys. Rev. **166**, 703 (1968).

[3] A. B. Pippard, *The Elements of Classical Thermodynamics* (Cambridge University Press, New York, 1957), p. 89.

[4] Derived using standard thermodynamic expressions. For example, J. C. Slater, *Introduction to Chemical Physics* (McGraw-Hill Book Co., New York, 1939).

[5] J. D. Barnett and C. D. Bosco, J. Appl. Phys. **40**, 3144 (1969).

Photocurrent and Thermally Stimulated Current Excitation Spectra in Cubic ZnSe Crystals

FAHD G. WAKIM

Itek Corporation, Lexington, Massachusetts 02173

(Received 15 August 1969; in final form 16 October 1969)

Several materials are known to exhibit a peak in the photocurrent spectral response at the band edge.[1,2] Under certain conditions, the peak may be very sharp, such that it defines sufficiently the bandgap energy of the materials. These conditions are a very rapid increase of the absorption constant at the band edge and a very high surface-to-volume ratio of recombination rates.[3] The free-carrier diffusion length must also be small compared to the sample dimensions. The purpose of this paper is to show that thermally stimulated current (TSC) excitation spectra also may exhibit a very sharp peak at the band edge. In such cases, an alternate means for defining the bandgap energy is provided.

The results presented here were obtained from cubic ZnSe crystals grown in this laboratory by a vapor transport technique described elsewhere.[4] Rectangular wafers approximately 5×4×0.6 mm were cut from the parent boule, and indium–gallium alloy
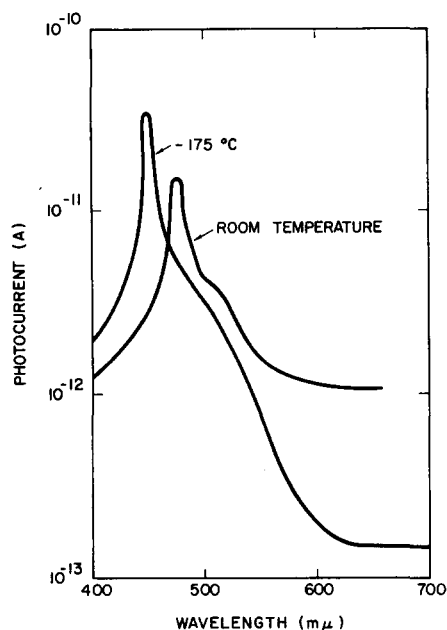

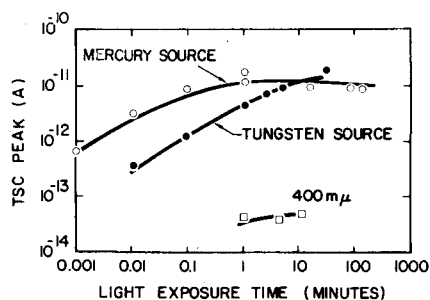FIG. 1. Photocurrent excitation spectra at 100° and 300°K.

FIG. 2. Height of the 158°K TSC peak as a function of exposure time (fixed intensity). Upper curves: 450-mμ light; the mercury source was a higher intensity than the tungsten source. Lower curve: 400-mμ light, same intensity as 450-mμ tungsten light.

contacts were applied to opposite ends of the wafers such that the current flow was transverse to the direction of the incident light. The *I–V* characteristics were ohmic over the entire voltage range investigated (to over 1000 V). The dark resistivities ranged between 10^{10} and 10^{12} Ω-cm. The approximate concentration of impurities detected by emission spectrographic analysis was Cu–5, Mg–1, Fe–2, Mn–3, Al–1, Si–8, and Ca–1, in parts per million. Light excitation was provided by a Bausch and Lomb high-intensity grating monochromator with a tungsten lamp. Light intensity was monitored by a thermocouple detector. When a very high-intensity light was needed (e.g., TSC saturation studies), the tungsten lamp was replaced by a high-pressure mercury lamp. Current measurements were made with a Keithly picoammeter by applying a constant 23 V across the crystal.

Photocurrent spectral response curves are shown in Fig. 1. At 100°K, a sharp peak appears at about 450 mμ (2.75 eV); this peak shifted to 475 mμ (2.60 eV) at 300°K in agreement with Bube.[1] The results above show a shift of 0.15 eV in the peak position when the temperature is changed from 100° to 300°K. This compares with the value of 0.134 eV obtained from the optical absorption data of Hite *et al.*[5] by plotting the energies at which $\alpha = 100$ cm^{-1} vs temperature and extrapolating to 300°K.

A shoulder is observed in the spectral distribution at about 520 mμ which can be due to some impurity such as copper. Stringfellow and Bube[6] found that copper in ZnSe introduced a shoulder in the photocurrent spectral distribution at about 2.5 eV (500 mμ) and two photoluminescence emission bands. The peak which they observed at the band edge was not as sharp as those we observed.

Several explanations have been proposed to account for the presence of a photocurrent peak at the band edge. The possibility that the decrease of photocurrent at wavelengths shorter than the band edge is due to an increase in a bimolecular recombination rate caused by the higher density of charge carriers generated close to the surface may be ruled out in this case. The photocurrent was found to be directly proportional to the light intensity, indicating that bimolecular recombination was not significant. The model presented by DeVore,[3] which depends on a high ratio of surface-to-volume recombination rates in combination with the variation of the spacial distribution of absorbed light with wavelength to produce the peak, is believed to be the most likely explanation for the present case.

Two peaks were observed in thermally stimulated current (TSC) and thermoluminescence (TL) curves at 118° and 158°K. The 158°K peak was the more prominent and corresponded to a trap depth of 0.38 eV below the conduction band as determined from analysis of the initial rise of the TSC peak. This agrees with the trap depth reported by Stringfellow and Bube.[6]

Figure 2 shows the magnitude of the 158°K TSC peak as a function of total exposure to 450-mμ light (constant intensity). The sample was illuminated at liquid-nitrogen temperature for different exposure times and then heated to 183°K to observe